J. Membrane Biol. 71, 173–182 (1983)

The Journal of
Membrane Biology

A Kinetic Study of the Opening and Closing Properties of the Hemocyanin Channel in Artificial Lipid Bilayer Membranes

G. Menestrina, D. Maniacco*, and R. Antolini

Dipartimento di Fisica, Libera Università degli Studi di Trento, 38050 Povo (TN), Italy

Summary. The kinetics of the hemocyanin channel conductance transitions in black lipid membranes have been studied in two different ways. In one method, voltage-jump current-relaxation experiments were performed with membranes containing many channels ($10^2 \div 10^4$). The steady-state conductance-voltage curves obtained are S-shaped and the slow kinetic processes (1–100 sec) for the approach to steady-state can be fitted by three exponentials. The three time constants were found to depend on the actual applied voltages, but not on the past history (preconditioning voltages). In the other method, membranes with one single channel were used and the spontaneous discrete fluctuations of conductance at constant voltage were analyzed. Slow fluctuations occur between four conductance levels with the lower ones preferred at high positive voltages. The voltage dependence of the conductance of each level and of the transition rates has been measured. A tentative model for the gating mechanism is suggested, which associates each conductance level to a configurational state of the channel and considers the transitions between them as a Markow jump process.

Key words hemocyanin channel · planar bilayer membrane · multistate transitions · channel kinetics

Introduction

Hemocyanin are respiratory copper proteins of large molecular weight representing more than 90% of the proteic content of the hemolymph of a number of invertebrates [26]. Following the finding that the hemocyanin extracted from the keyhole limpet *Megatura crenulata* markedly increases the ionic conductance of bilayer lipid membranes [21], evidence has been obtained that at least three different molluscan hemocyanins form ionic pores in lipid bilayers [1, 3, 14].

Little so far is known about the structure of the channel until now. Hemocyanin molecules in solution at pH 7.0 are hollow cylinders with length and external diameter both about 30 nm [26], but the channel is probably due to a different structure. An electron-microscopy study on the interaction of keyhole limpet hemocyanin with different artificial lipid systems has been reported recently [13] and suggests that the possible channel-forming structure is a proteic annulus about 7 nm in diameter, protruding into the solution for about 3 nm and with a central pool of staining of 2-nm diameter, which may be related to the ionic pathway.

Two major problems arise from the study of the ion conductance through the hemocyanin channel, as well as any other: which gating process is able to modulate the conductance and by which conduction process do ions move across the open pore? Both aspects have been investigated for the channel formed by the *Megatura crenulata* hemocyanin. The open channel was found to be permselective to cations without discrimination among them [2]. Its conductance is a sublinear function of the salt concentration and shows a pH dependence that reminds the titration of the protein in free solution [16]. Binding of divalent cations to the hemocyanin channel [15], as well as to the free protein [9] has been found. All these properties have been explained assuming that the channel bears a negative fixed charge and a part of this charge resides in a negative site which can bind divalent cations as well as small monovalent cations like Li^+ and H^+ [17]. Furthermore the voltage-dependent conductance of many-channel membranes was demonstrated to arise from two characteristics of the individual channels: fluctuations between at least four conductance levels with voltage-dependent dwell time in

* *Present address:* Lab. für Biochemie, E.T.H., CH-8092 Zürich, Switzerland.

0022-2631/83/0071-0173 $02.00

each state and voltage-dependent conductance of the single levels themselves [12].

In this paper we dedicate our attention to the above-mentioned discrete conductance changes reporting on their kinetics. Two methods have been followed: voltage-jump current-relaxation experiments with many-channel membranes and analysis of discrete spontaneous conductance fluctuations with single-channel membranes. The time-course of conductance fluctuations in a single channel shows a rather complicated pattern of transitions; nevertheless we try to consider only slow fluctuations determining the voltage dependence of their transition rate constants as well as the voltage dependence of the conductance of each single level. From these data, assuming a tentative four-states model for the hemocyanin channel and according to the general treatment suggested by Neher and Stevens [20] for multistate systems, we are able to predict the observed voltage dependence of both steady-state conductance and slow relaxation times of the many-channel membranes. The interest of this kind of approach to the hemocyanin channel has been recently pointed out in a review by Latorre and Alvarez [11], and it is worth noting also that several natural channels such as Na^+-channel of nerves [4], ACh receptor channel [8] and K^+ channel of sarcoplasmic reticulum [10], have been found to be multistate channels.

Materials and Methods

Black lipid membranes (BLM) were obtained by the usual technique [24] using oxidized cholesterol prepared by us following the procedure of Tien [25] with cholesterin and *n*-octane (Fluka puriss.p.a.).

The Teflon sept, separating the two compartments had a circular hole of about 1-mm diameter.

Control experiments were performed also on painted phosphatidylcholine (PC) *n*-decane, 50 mg/ml, BLM and on bilayers obtained by the apposition technique [19] with a mixture of 50% phosphatidylethanolamine (PE) and 50% phosphatidylserine (PS). PC and PE were from P.L. Biochemicals, more than 99% pure, and PS was a gift of Dr. A. Gorio, Fidia Research Laboratories, Abano Terme. All experiments were performed at room temperature, ranging from 20 to 23 °C, using electrolytic solutions of 0.1 M KCl (Carlo Erba RPE) buffered at pH 7 with 10 mM Bistris (Sigma). One mM EDTA was added to the solution to eliminate traces of divalent ions which were shown to strongly influence channel properties [15].

Megatura crenulata hemocyanin, A grade in 50% glycerol, was purchased by Calbiochem and stored at −20 °C. When the BLM was completely formed, small amounts of a 3.3 mg/ml stock solution were added to the bathing solution, on one side only, reaching a final concentration of about 10 μg/ml for many-channel membranes and 0.2 μg/ml when single channels were expected to appear. Membrane conductance was measured under voltage-clamp conditions, where the voltage was supplied by a function generator or a variable battery and the bilayer was connected to the external circuit by four Ag/AgCl electrodes. Membrane current and voltage were measured with current-to-voltage transducer and differential amplifier, respectively. Very low bias operational amplifier (Analog Devices 515-K) were used and the feedback loop for the current-to-voltage conversion was a $10^8\ \Omega$ resistor shunted with a 50-pF capacitor. Both output signals were recorded on a chart recorder and on an FM magnetic tape recorder.

During the experiments with many-channel membranes the $I-V$ converter was substituted by a commercial electrometer (Keithley 616) in order to change the current range more easily.

Single-channel records have been analyzed off-line connecting the FM recorder to a SILENA S-27 multichannel analyzer in the Pulse Height Amplitude mode (PHA) through a linear switch (SILICONIX DG 201) that chopped the signal at 1000 Hz. Current resolution was 0.1 pA per channel. The result of PHA analysis is a spectrum containing a number of peaks whose positions represent one current level and whose areas represent the fraction of time spent by the system on that level [14].

In many-channel experiments, the actual current values were corrected for a continuous increase due to a virtually irreversible channel-formation process. This was made starting the measurements when the number of channels was such that the current drift could be considered small and linear and therefore it could be easily subtracted. The protein-containing compartment was taken as the reference for the current and voltage signs.

Protocol for Single-Channel Experiments

As shown in Ref. [12], single hemocyanin channels exhibit several conductance values for positive potentials, but only one for negative applied voltages. This fact rules out the possible interpretation that the several conductance levels observed at positive voltage (*see*, for example, Fig. 4) are due to several different channels, and allow us to make single-channel experiments with the following procedure:

a) Protein incorporation was carried out clamping the membrane at −50 mV so that the channel always appeared in its maximum conductance state.

b) Once a channel was formed (in our conditions a current jump of about 170 pS, a factor 10 above the bare membrane, was observed), the solution of the protein-containing compartment was quickly, but gently, substituted with a fresh protein-free solution in order to prevent further incorporation. The perfusion apparatus we used was similar to that described by Miller and Rosenberg [18], who give an efficiency of more than 99%. With this procedure, single-channels lasting some hours have been obtained.

c) Current records were obtained applying voltage steps of different amplitudes, in clamp conditions, lasting about 10 min. Between one pulse and the other the channel was kept to −50 mV for some seconds, in order to completely open it and to control the total conductance of the system so that it did not change during the measurement, i.e. the bilayer always contained only one channel.

The Multistate Model

Previous work on the gating properties of the hemocyanin channel suggested the existence of a multistate conformational mechanism [12]. Our intention here is to outline a model of channel gating following the general treatment described by Neher and Stevens [20] where channels are considered as multistate systems which can exhibit transitions according to Poisson processes. In this section we set forth the postulates upon which the model rests and we give the equation that expresses the average response to perturbations in terms of state conductances and transition rates. The assumptions of the model are:

1) The channel is inserted into the bilayer with a fixed orientation.

2) Channels are considered identical and mutually independent entities.

3) Each channel has n distinguishable states, associated to n conductance levels.

4) Transitions between these states are Poisson processes, i.e. the probability of going from state i to j during the interval Δt approaches $a_{ij}\Delta t$ as Δt approaches 0. For such a process the distribution of dwell times for each state is expected to be exponential.

5) The a_{ij}, which represent the transition rates, are assumed to depend on several factors such as voltage, temperature, type and concentration of the electrolyte, etc., but not on time or the past history of states occupied. They can be conveniently arranged in a matrix $\mathbf{A}(\mathbf{V})$, where the vector $\mathbf{V}$ contains all the relevant variables upon which $\mathbf{A}$ depends. In this paper only the voltage-dependence of $\mathbf{A}$ will be investigated.

The dynamics of the channel will be described by the state vector $\mathbf{x}(t)$ whose j-th entry is the probability to find the channel in state j at time t. A completely standard mathematical treatment of the kinetics of multistate channels [6] leads to the following equation relating the state vector at time t with that at time zero, once fixed $\mathbf{V}$:

$$\mathbf{x}(t)=e^{\mathbf{B}t}\,\mathbf{x}(o) \tag{1}$$

where the matrix $\mathbf{B}$ is simply related to the transition rate matrix $\mathbf{A}$ by

$$b_{ij}=a_{ji}, \quad (j\neq i)$$

and

$$b_{ii}=-\sum_{i,\,l\neq i} a_{il}, \quad (i=1,\ldots,n). \tag{2}$$

Equation (1) may be more conveniently rewritten, according to the spectral theorem of linear algebra, as a power series:

$$\mathbf{x}(t)=\sum_i e^{\lambda^{(i)}\cdot t}\,\mathbf{E}^{(i)}\,\mathbf{x}(o) \tag{3}$$

where the $\lambda^{(i)}$ are the eigenvalues of $\mathbf{B}$ and the $\mathbf{E}^{(i)}$ are the projectors onto the eigenvectors corresponding to the $\lambda^{(i)}$. These quantities can be obtained by standard diagonalization techniques applied to $\mathbf{B}$. Because of the definition of $\mathbf{B}$ all its eigenvalues are less or equal to zero at least one being null. Therefore we put $\lambda^{(1)}=0$.

The mean conductance $\bar{\gamma}$ of the channel may be expressed as

$$\bar{\gamma}(t)=\gamma\cdot\mathbf{x}(t) \tag{4}$$

where γ is a vector whose component γ_i represent the conductance of the i-th state of the channel.

Making use of Eq. (3), Eq. (4) becomes:

$$\bar{\gamma}(t)=\gamma\cdot[\mathbf{E}^{(1)}\,\mathbf{x}(o)+\sum_i e^{\lambda^{(i)}\cdot t}\,\mathbf{E}^{(i)}\,\mathbf{x}(o)],$$

$$(i=2,\ldots,n) \tag{5}$$

where the first term between parentheses represents the steady-state part of the solution whereas the summation represents the transient one, $-1/\lambda^{(i)}=\tau_i$ being the time constants of the process.

Results

Voltage-Jump Current-Relaxation Experiments

When small amounts of *Megatura crenulata* hemocyanin are added to the reference side of a black lipid bilayer clamped at a negative voltage, the membrane conductance increase in discrete steps of practically constant size which have been attributed to the formation of open channels [1].

When the voltage across a many-channel membrane is suddenly changed the current quickly follows it then it keeps flat or slowly relaxes to lower values depending on the applied voltage (Fig. 1*a*). The time course of the current during the relaxation processes, as it results from Fig. 1*c* and *d*, can be reasonably well described by the sum of three exponential components implying a kinetic scheme for the channel closing with at least three steps [22].

The analysis of each current time course allows us to obtain both the steady-state conductance and the time constants of the relaxation. Steady-state conductances have been normalized dividing the actual conductance for that at -50 mV, that is the conductance of the open pore. When plotted against the applied potential, these follow a sigmoidal curve (Fig. 2) whose shape does not depend on the number of channels in the membrane (results from different membranes with different total number of channels are superimposed in Fig. 2), in agreement with previous findings that the channels are mutually independent.

The three time constants as a function of the applied potential are shown in Fig. 3*a*. All the relaxation times are different from zero only in the region of positive potentials and at least the two slower values show well-pronounced maxima located in the same voltage range where the steady-state conductance presents its maximum negative slope.

Furthermore the time constants seem not to depend on the total number of channels, at

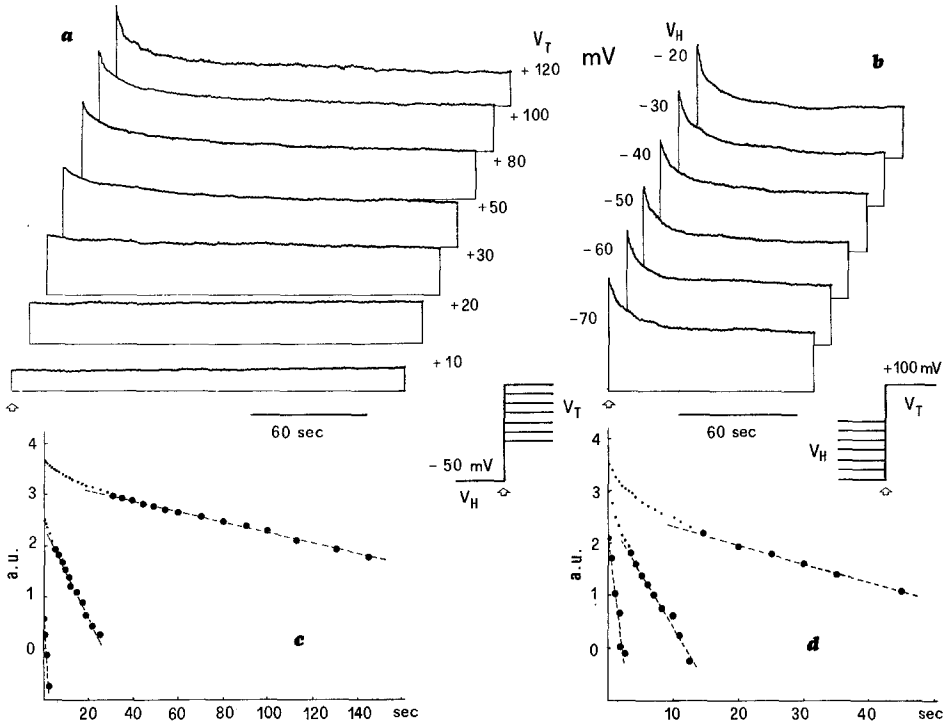

Fig. 1. Current relaxation after voltage jumps from holding voltages V_H to test voltages V_T. (*a*) Variation in test voltages. The holding voltage was -50 mV in all cases. (*b*) Variation in holding voltages. The test voltage was $+100$ mV in all cases. (*c*), (*d*) Half-logarithmic plots of digitized traces representative of experiments (*a*) and (*b*), respectively. The points of the upper part are the half logarithmic plot of the relaxation amplitude $I-I^*$ versus t, where I^* is the steady-state current. A single exponential fitting accounts only for the last part of the Figure (largest points), and represents the slow relaxation process. Faster relaxation processes have been resolved (lower parts) with the same procedure after subtracting the slower ones. All the experimental curves could be fitted with the function

$$I=I_\infty+I_1\,e^{-t/\tau_1}+I_2\,e^{-t/\tau_2}+I_3\,e^{-t/\tau_3}.$$

Since only time constants are under investigation current is expressed in arbitrary units in the Figure

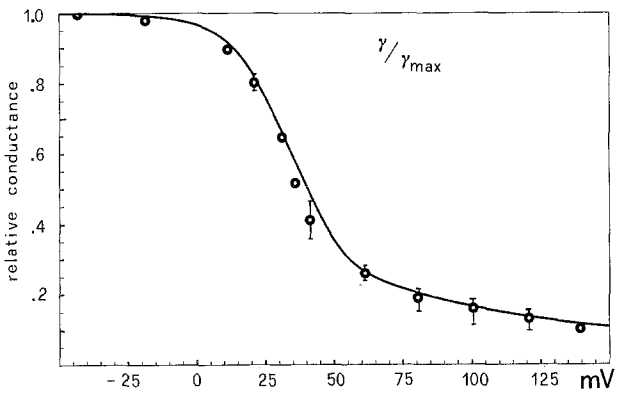

Fig. 2. Steady-state conductance-voltage relation. Compiled data from four membranes, with each set normalized to its maximum conductance. The solid curve is the prediction of the model presented through the text

least in the limit of the large error bars shown in Fig. 3. These are due to the fact that while repetition is good during the same measurement, some difficulties were encountered when we tried to compare data from different membranes. The same kind of difficulties have been reported also in similar studies on the EIM channel [7].

A series of experiments have been done in order to verify if relaxation times depend on the starting potential or, in other words, if the process possesses some kind of "memory". The results are shown in Figs. 1*b* and 3*b* and demonstrate, in the limits discussed above, that the relaxation times are independent on the preconditioning potential and depend only on the actual potential.

Discrete Conductance Fluctuations in Individual Channels

Records of current time-course through individual hemocyanin channels in membranes clamped at different voltages have been obtained, following the procedure described in Materials and Methods, and a few examples are shown in Fig. 4. We can immediately observe

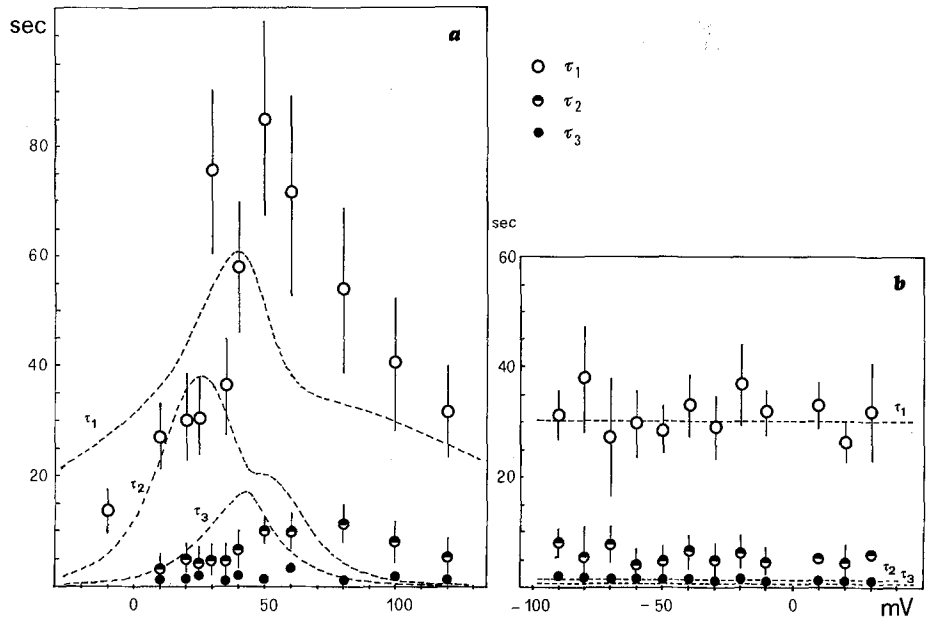

Fig. 3. Voltage dependence of relaxation time constants. (*a*) Variation in test voltage. The relaxation times were measured, under the conditions of Fig. 1(*a*), by a least-square fitting method as shown in Fig. 1(*c*). Each point represents the mean of 4 to 8 determinations taken from three different membranes. Error bar is twice the S.D. The dashed lines represent the theoretical values of the τ_i computed as $-\frac{1}{\lambda(i)}$ wwhere $\lambda^{(i)}$ are the eigenvalues of the matrix **B** defined in the text. (*b*) Variation in holding voltage. The relaxation times were measured under the conditions of Fig. 1(*b*). The experimental points which are the mean of 3 to 4 determinations on one single membrane, show the independence of the time constants from the voltage from which a jump is made. Dashed lines and error bars have the same meaning as in part (*a*)

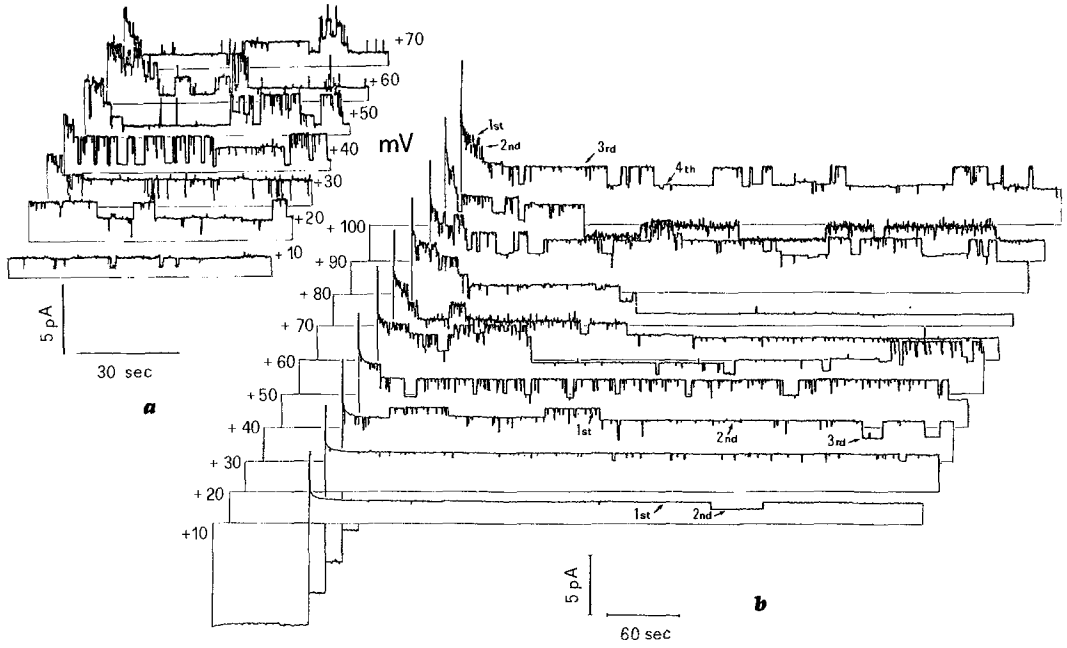

Fig. 4. Current fluctuations in a single-channel membrane. Current records after a jump from −50 mV to the indicated potential in membranes containing only one channel. (*a*) Folded membranes of PE/PS; (*b*) painted membranes of oxidized cholesterol. After the jump the channel is in the open state, then fluctuations between several levels occur. The four fundamental levels have been indicated with arrows and labeled 1st, 2nd, 3rd and 4th in order of decreasing conductance

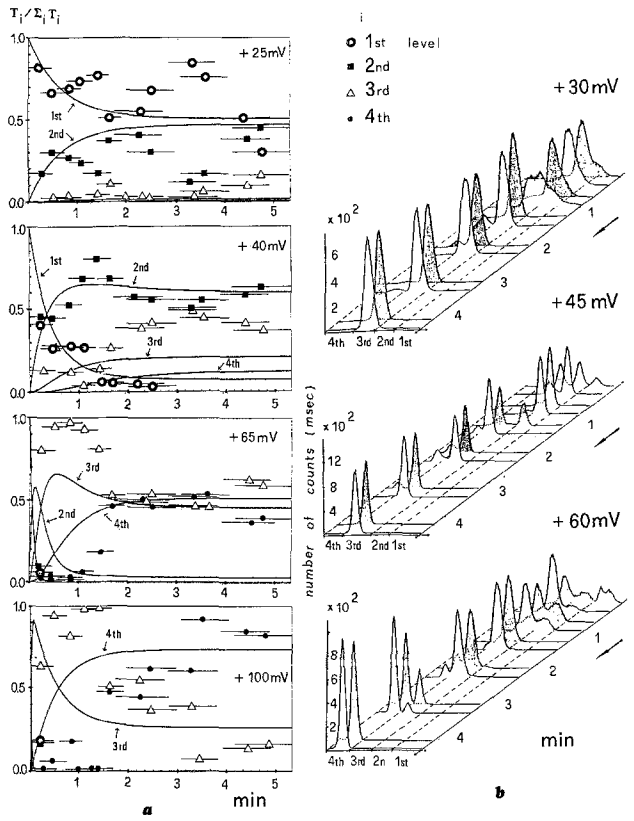

Fig. 5. Time evolution of the state vector. Current records of the kind shown in Fig. 4 were analyzed with an MCA in PHA mode (*see* Materials and Methods). Spectra were taken during successive periods of time; six 30-sec intervals and six 60-sec intervals were analyzed. Three examples of the spectra obtained are shown in part (*b*) and illustrate the time evolution of the population of the different levels, at the indicated potential. Normalized data are reported in the diagrams of part (*a*) where each point represents the fraction of time spent by the channel in a certain level, during a measuring time indicated by the horizontal bar. In other words if we indicate with τ_i the area under the *i*-th peak of one spectrum of part *a* each point of part *b* represents $\tau_i/\sum_i \tau_i$. The solid lines represent the theoretical time course of $x_i(t)$ (Eq. 5 of the text). Measurements from two or three different membranes have been averaged

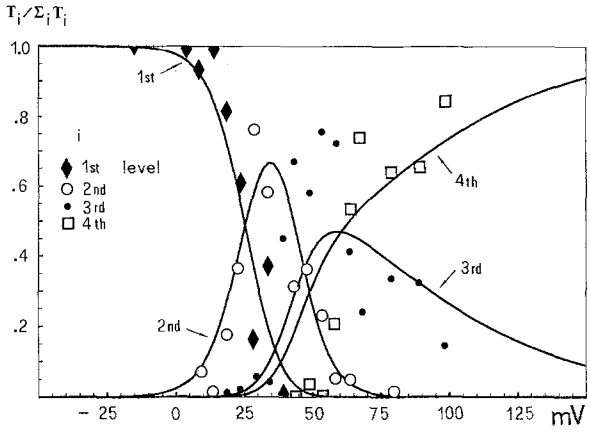

Fig. 6. Voltage dependence of the steady-state vector. PHA has been performed on the steady-state part of current records of Fig. 4. Steady-state conditions are claimed after a period corresponding to at least three times the slowest time constant of Fig. 3(*a*). Output spectra were normalized as in Fig. 5(*a*) to give the fraction of time spent in each level by the channel in steady conditions and reported in the Figure. Average data from two to three different membranes. Solid lines represented the four components of the state vector $x_i(t)$ computed for $t = 350$ sec

from the Figure that relaxations, till now studied in many-channel membranes, arise from transitions of the channel between several conductance levels. Immediately after the potential is changed, starting from its more conductive state, the channel begins oscillating back and forth between different conductance levels up to a steady state in which the lower levels are more and more preferred as the membrane potential is increased in the positive range.

The experiments with single-channel fluctuations allow us to obtain the state vector both in steady conditions and during the transient evolution by measuring the dwell times in each conductance level. This was done by feeding long records of current, similar to those of Fig. 4, into a pulse height analyzer and recording the time spent in each 0.1 pA window on the current axes as described in Materials and Methods.

Figure 5 represents a few examples of this kind of study during the relaxation process which follows a stepwise increase of the applied voltage from -50 mV to different final voltages. In part *b* of the Figure we have directly reproduced the outputs of the analyzer whereas in part *a* the same kind of data were normalized giving the evolution of the fraction of time spent in each level, that is of the components of the state vector.

Applying the same kind of analysis to the steady part of the current records we could measure the dependence of the steady-state vector on the applied voltage. This is shown in Fig. 6 where we have reported normalized data which give the probability of occupancy of each level *vs.* potential.

Single-channel current records were also analyzed by hand to give both the conductance of each state and the transition rates between them. In Fig. 7 the voltage dependence of the conductance of each individual level, that is of the components of what we call the conductance vector, is shown. At least the first three

levels are non linear, confirming previous results [12].

Transition rates were computed as [7]:

$$a_{ij}=\frac{n_{ij}}{\sum_{\mu} t_i(\mu)} \tag{6}$$

where n_{ij} are number of transitions from state i to j and $t_i(\mu)$ is the μ-th dwell time in state i.

Some problems arose in the determination of n_{ij} and t_i due to the fact that two kinds of fluctuations with different time scales were observed (*see inset* of Fig. 8). In a first analysis we considered all the transitions, but this led to time constants of the order of seconds, about ten times too fast compared both to many-channel and single-channel kinetics. In a second analysis we considered only the slow transitions which occur between the four more evident levels and the results we obtained are shown in Fig. 8 where transition rates have been reported as a function of the applied voltage in a half-logarithmic plot and fitted by straight lines. In order to test if the transitions between different conductance levels are Poisson processes, we have built up the distribution of dwell times for each state and a few examples are shown in Fig. 9. Each histogram shows the cumulative sum of the number of events of duration longer than t_d plotted as a

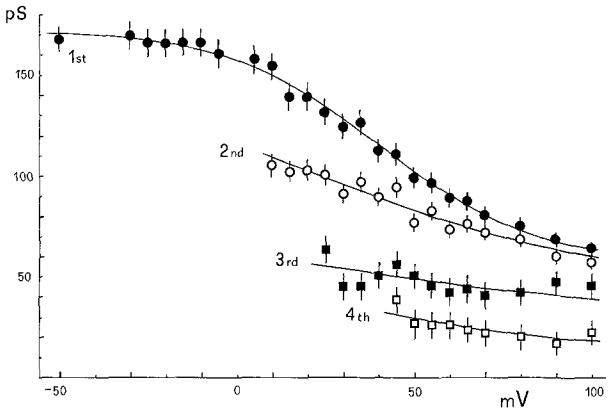

Fig. 7. Voltage-dependence of the conductance of the four discrete levels of a single hemocyanin channel. Points are mean values of measurements on two to three membranes. Solid lines are least-squares fit to the points with Eq. (9)

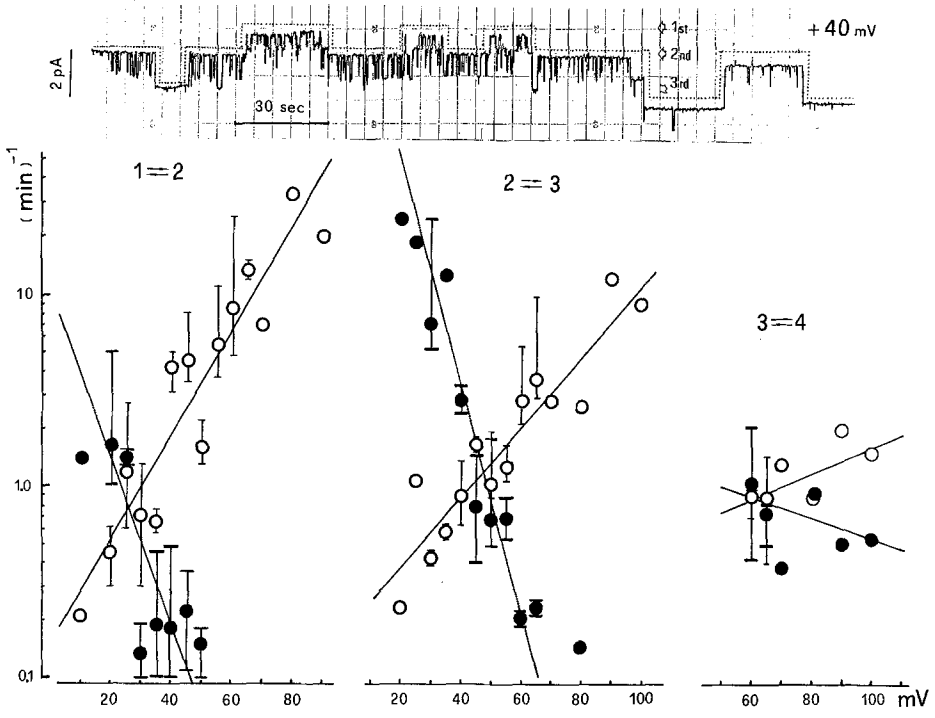

Fig. 8. Voltage dependence of rate constants. The effect of membrane voltage on single-channel rate constants for slow transitions between the four allowed states is presented in a semilogarithmic plot. Slow transitions have been chosen as shown by the dotted line in the inset. The rate constants were computed as indicated in Eq. (6) with a total number of transitions and a total time accumulated from measurements on 1 to 3 different membranes. A mean of 6 transitions and 9 time intervals has been used. Errors bars cover the interval between the minimum and the maximum value observed in different membranes, while points without bars refer to single determinations. The straight lines shown in the figure are least-squares fit to the experimental points. Each point was weighted by the number of transitions used to calculate it

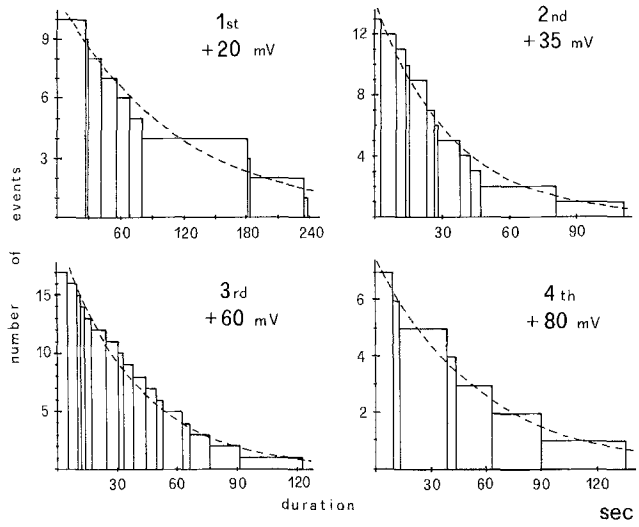

Fig. 9. Accumulated distribution of dwell times. Each plot shows the histogram of the number of individual dwell times which are longer than the time indicated by the abscissa and is computed for the level and the voltage indicated. The dashed lines are least-squares fit with an exponential function

function of t_d. We have obtained histograms of this kind for several membrane voltages, with three different membranes and all these distributions have been fitted with exponential curves with a correlation coefficient of 0.95 ± 0.03.

Discussion

It is worthwhile starting this section by reviewing and discussing the five postulates upon which our multistate conformational model for the gating properties of the channel is based. For it, we will make use of the experimental results presented in this paper as well as of reference data.

The first assumption, regarding the orientation of the channels in the bilayer, is supported by the asymmetry of the $G-V$ curves as was already discussed elsewhere [11]. The second assumption, i.e. the independent gating of the channels, is consistent with all experimental facts till now known [11]. In particular, in this work we have shown that both $G-V$ curves and relaxation times do not depend on the number of channels in the membrane. The fact that all channels are identical is a reasonable assumption but not strictly right; in fact single-channel conductances, for example, show a reproducible but relatively wide distribution around a mean value [2].

The third assumption is more critical, since only conductance levels have been directly measured and their biunivocal association to channel states is therefore arbitrary, and by means of kinetic tests we can only verify its consistence.

The last two assumptions concern the transitions between different states of the channel. We have shown in Fig. 9 that the distribution of dwell times can be well fitted by single exponentials as it should be if the switching over two conductance states may be regarded as a Poisson process. We have also shown that in membranes containing many channels the relaxation times are unaffected by the initial voltage, which is consistent with the fifth hypothesis that the channel is memoryless. A physical interpretation of the above-outlined model may be obtained looking at the membrane conductance changes as reflecting channel gating by macromolecules driven between different conformational states by membrane voltage. Thus our system can be represented by the diagram

$$c_1 \underset{a_{21}}{\overset{a_{12}}{\rightleftarrows}} c_2 \dots c_i \underset{a_{ji}}{\overset{a_{ij}}{\rightleftarrows}} c_j \dots c_{n-1} \underset{a_{n(n-1)}}{\overset{a_{(n-1)}}{\rightleftarrows}} c_n \tag{7}$$

where c_i are the permitted conformations and only transitions between neighboring states are allowed.

Now, we can make use of the model in order to predict a number of experimental results. Single-channel measurements permit us to fill in the transition rate matrix **A** as well as the conductance vector γ. The first information gathered from the experimental records regards the number N of discrete conductance levels that are the dimensions of **A** and γ. Looking only at the slow transitions, as pointed out in the Results, it seems likely that the channel jumps between four more evident levels. Therefore we have assumed that the allowed states of the channel are four.

While keeping in mind that both **A** and γ may depend on several parameters, in this work we concentrate only on their voltage dependence and thus we kept constant all other conditions. As shown in Fig. 8 the transition rates can be represented as exponential functions of membrane potential, so we can write:

$$a_{ij} = \nu_{ij} \exp\{\eta_{ij}(V - V_{oij})\}. \tag{8}$$

In the half-logarithmic plots of Fig. 8 the two transition rates a_{ij} and a_{ji} have been fitted

by straight lines whose slopes are η_{ij} and η_{ji} and whose intersection point is at (V_{oij}, ν_{ij}), so we have $\nu_{ij}=\nu_{ji}$ and $V_{oij}=V_{oji}$.

In the framework of the gating model, the observed exponential dependence of the rate constants means that the free energy barriers between the different conformations of the channel depend linearly on the applied voltage. Such a dependence reflects the interaction of the electric field with charged groups or permanent electric dipoles of the channel-forming protein. A detailed discussion of the fundamental electric-field effects on macromolecular systems with regard to the physicochemical nature of voltage-dependent biological processes may be found in Ref. [23].

The two slopes η_{ij} and η_{ji} are in general different, even in the modulus, but for the sake of simplicity in our model we have assumed that $\eta_{ij}=\eta_{ji}$ as for example in Ref. [7]. This corresponds to the particular case in which both states of the channel change in energy to the same extent with the applied field [7]. The loss of information due to this assumption would be more apparent in Figs. 3 and 5, but appropriate tests indicated that dropping this assumption does not substantially improve the fit.

Turning to the voltage dependence of the conductance vector γ, expressed by the experimental points shown in Fig. 7, we can observe that, at least for the first level, the data clearly follow a sigmoidal curve. The significance of this curve has been recently investigated in two works [5, 17].

Due to experimental difficulties, only the voltage dependence of the first level was studied in detail; in this work we fitted all the levels with the same following empirical equation:

$$\gamma_i = G_i + \Delta G_i/(1+\exp K_i(V-V_{oi}^*)) \qquad (9)$$

where G_i and ΔG_i represent, respectively, the low asymptote and the difference between high and low ones.

The best fit parameters we obtained have been reported in the Table. Once we determined the voltage dependence of both **A** and γ, we were in a position to test the model. This has been done numerically with the aid of a computer. The matrix **B** was deduced from **A** (Eq. 5), and standard diagonalization procedures give the $\lambda^{(i)}$ and $\mathbf{E}^{(i)}$ as a function of voltage. Therefore the theoretical curves representing the voltage dependence of the relaxation times, of the components of the state vector and of the mean conductance of the channel could be plotted and the results could be compared with experimental data as shown in Figs. 3, 6 and 2, respectively. The model allows us to evaluate also the time evolution of the state vector; in Fig. 5 a few examples of such calculations are compared with the measured values.

Table. Input parameters for the multistates conformational model

A: Transition rates matrix

$a_{ij}=\nu_{ij}\{\exp \eta_{ij}(V-V_{oij})\}$

$\nu_{ij}=\nu_{ji}=\nu \qquad V_{oij}=V_{oji}=V_o \qquad \eta=\frac{1}{2}(\eta_{ij}-\eta_{ji})$

	$C_1 \rightleftarrows C_2$	$C_2 \rightleftarrows C_3$	$C_3 \rightleftarrows C_4$
ν (sec^{-1})	0.013	0.020	0.015
η (mV^{-1})	0.073	0.075	0.013
V_o (mV)	25.5	47	60.5

Parameters obtained by least-square fitting to the points of Fig. 8 with the indicated equation. The values of η are means of η_{ij} and $-\eta_{ji}$. Owing to the small number of events observed, the mean values reported in the Table should be taken as merely suggestive, as it straightforth appears examining the error bars of the points in Fig. 8.

γ: Conductance vector

$\gamma_i=G_i+\Delta G_i/\{1+\exp K_i(V-V_{oi}^*)\}$

	1st	2nd	3rd	4th
G (pS)	57.3	44.8	30.3	13.9
ΔG (pS)	115.2	116.9	53.4	40.7
K (mV^{-1})	0.047	0.023	0.020	0.034
V_o^* (mV)	40.7	18.7	18.4	35.6

Least-square fitting parameters obtained by the points of Fig. 7.

In spite of the complexity of the channel behavior and the strong approximation of the model the accordance between predictions and data are rather satisfying.

With this work we have tried to give a piece of information on the kinetics of the hemocyanin channel, filling a gap which obstructed the formulation of models on the molecular changes involved in the stepwise slow relaxation of the channel [11].

This work was supported in part by grants from the Ministero della Pubblica Istruzione and Consiglio Nazionale delle Ricerche. We would like to thank Prof. P. Lauger and Dr. L. Guzman for comments on the manuscript and Mrs. E. Agostini and Mr. G. Chini for technical assistance.

References

1. Alvarez, O., Diaz, E., Latorre, R. 1975. Voltage-dependent conductance induced by hemocyanin in black lipid films. *Biochim. Biophys. Acta* **389**:444–448
2. Antolini, R., Menestrina, G. 1979. Ion conductivity of the open keyhole limpet hemocyanin channel. *FEBS Lett.* **100**:377–381
3. Antolini, R., Menestrina, G. 1981. Effects of *Aplysia* hemocyanin on the conductance of oxidized cholesterol black lipid membranes. *Biochim. Biophys. Acta* **649**:121–124
4. Armstrong, C.M., Bezanilla, F. 1977. Inactivation of the sodium channel. II. Gating current experiments. *J. Gen. Physiol.* **70**:567–590
5. Cecchi, X., Alvarez, O., Latorre, R. 1981. A three-barrier model for the hemocyanin channel. *J. Gen. Physiol.* **78**:657–681
6. Colquhoun, D., Hawkes, A.G. 1977. Relaxation and fluctuations of membrane currents that flow through drug-operated ion channels. *Proc. R. Soc. London, B* **199**:231–262
7. Ehrenstein, G., Blumenthal, R., Latorre, R., Lecar, G. 1974. Kinetics of the opening and closing of individual excitability-inducing material channels in a lipid bilayer. *J. Gen. Physiol.* **63**:707–721
8. Hamill, O.P., Sakmann, B. 1981. Multiple conductance states of single acetylcholine receptor channels in embryonic muscle cells. *Nature (London)* **294**:462–464
9. Klarman, A., Shaklai, N., Daniel, E. 1972. The binding of calcium ions to hemocyanin from *Levantina hierosolima* at physiological pH. *Biochim. Biophys. Acta* **257**:150–157
10. Labarca, P.P., Miller, C. 1981. A K^+-selective, three-state channel from fragmented sarcoplasmic reticulum of frog leg muscle. *J. Membrane Biol.* **61**:31–38
11. Latorre, R., Alvarez, O. 1981. Voltage-dependent channels in planar lipid bilayer membranes. *Physiol. Rev.* **61**:77–150
12. Latorre, R., Alvarez, O., Ehrenstein, G., Espinoza, M., Reyes, J. 1975. The nature of the voltage-dependent conductance of the hemocyanin channel. *J. Membrane Biol.* **25**:163–182
13. McIntosh, T.J., Robertson, J.D., Ting-Beall, H.P., Walter, A., Zampighi, G. 1980. On the structure of the hemocyanin channel in lipid bilayers. *Biochim. Biophys. Acta* **601**:289–301
14. Menestrina, G., Antolini, R. 1979. A different kind of hemocyanin channel in oxidized cholesterol membranes. *Biochem. Biophys. Res. Commun.* **88**:433–439
15. Menestrina, G., Antolini, R. 1981. Effects of Ba^{2+} and Ca^{2+} on the conductance of the hemocyanin channel in black lipid membranes. *Period. Biol.* **83**:166–170
16. Menestrina, G., Antolini, R. 1981. Ion transport through hemocyanin channels in oxidized cholesterol artificial bilayer membranes. *Biochim. Biophys. Acta* **643**:616–625
17. Menestrina, G., Antolini, R. 1982. The dependence of the conductance of the hemocyanin channel on applied potential and ionic concentration with mono- and divalent cations. *Biochim. Biophys. Acta* **688**:673–684
18. Miller, C., Rosenberg, R.L. 1979. A voltage-gated cation conductance channel from fragmented sarcoplasmic reticulum. Effects of transition metal ions. *Biochemistry* **18**:1138–1145
19. Montal, M., Mueller, P. 1972. Formation of bimolecular membranes from lipid monolayers and a study of their electrical properties. *Proc. Natl. Acad. Sci. USA* **69**:3561–3566
20. Neher, E., Stevens, G.F. 1977. Conductance fluctuations and ionic pores in membranes. *Annu. Rev. Biophys. Bioeng.* **6**:345–381
21. Pant, H.C., Conran, P. 1972. Keyhole limpet hemocyanin (KLH)-lipid bilayer membrane (BLM) interaction. *J. Membrane Biol.* **8**:357–362
22. Schwarz, G. 1968. Kinetic analysis by chemical relaxation methods. *Rev. Mod. Phys.* **40**:206–218
23. Schwarz, G. 1979. Electric-field effects on macromolecules and the mechanism of voltage-dependent processes in biological membranes. *In:* The Neurosciences Fourth Study Program. F.O. Schmitt and F.G. Worden, editors. pp. 631–639. MIT Press, Cambridge, Mass.
24. Szabo, G., Eisenman, G., Ciani, S. 1969. The effects of the macrotetralide actin antibiotics on the electrical properties of phospholipid bilayer membranes. *J. Membrane Biol.* **1**:346–352
25. Tien, H.T. 1974. Bilayer Lipid Membranes (BLM): Theory and Practice. Marcel Dekker, New York
26. Van Bruggen, E.F.J., Wiebenga, E.M., Gruber, M. 1962. Structure and properties of hemocyanins. I. Electron micrographs of hemocyanin and apohemocyanin from *Helix pomatia* of different pH values. *J. Mol. Biol.* **4**:1–7

Received 17 March 1982; revised 9 July 1982